American Journal of Pathology, Vol. 163, No. 4, October 2003


# Oxidative Stress and Oval Cell Accumulation in Mice and Humans with Alcoholic and Nonalcoholic Fatty Liver Disease

Tania Roskams,* Shi Qi Yang,† Aymen Koteish,† Anne Durnez,* Rita DeVos,* Xiawen Huang,† Ruth Achten,* Chris Verslype,* and Anna Mae Diehl†

*From the Departments of Morphology and Molecular Pathology and Hepatology,* University of Leuven, Leuven, Belgium; and the Department of Medicine,† The Johns Hopkins University, Baltimore, Maryland*

**In animals, the combination of oxidative liver damage and inhibited hepatocyte proliferation increases the numbers of hepatic progenitors (oval cells). We studied different murine models of fatty liver disease and patients with nonalcoholic fatty liver disease or alcoholic liver disease to determine whether oval cells increase in fatty livers and to clarify the mechanisms for this response. To varying degrees, all mouse models exhibit excessive hepatic mitochondrial production of $H_2O_2$, a known inducer of cell-cycle inhibitors. In mice with the greatest $H_2O_2$ production, mature hepatocyte proliferation is inhibited most, and the greatest number of oval cells accumulates. These cells differentiate into intermediate hepatocyte-like cells after a regenerative challenge. Hepatic oval cells are also increased significantly in patients with nonalcoholic fatty liver disease and alcoholic liver disease. In humans, fibrosis stage and oval cell numbers, as well as the number of intermediate hepatocyte-like cells, are strongly correlated. However, cirrhosis is not required for oval cell accumulation in either species. Rather, as in mice, progenitor cell activation in human fatty liver diseases is associated with inhibited replication of mature hepatocytes. The activation of progenitor cells during fatty liver disease may increase the risk for hepatocellular cancer, similar to that observed in the Solt-Farber model of hepatocarcinogenesis in rats. *(Am J Pathol 2003, 163:1301–1311)***

In rodent models for hepatocarcinogenesis, small oval cells that express both hepatocyte and cholangiocyte markers accumulate in the liver before cancerous nodules develop.[1–4] Similar oval cell accumulation has also been described in human liver, close to hepatitis B-associated hepatocellular carcinoma,[5] in hepatoblastoma,[6] in regenerating liver,[7] and in cholestatic liver diseases.[8] We recently showed that putative progenitor cells accumulate in the livers of patients with chronic hepatitis C, an acknowledged risk factor for hepatocellular carcinoma.[9,10] Moreover, in those studies, a direct correlation between the oval cell response and the degree of hepatic inflammation was demonstrated, suggesting that inflammatory cytokines and the resultant oxidant stress play a role in the activation of human progenitor cells during chronic viral hepatitis.

Animal data indicate that oval cells are activated when oxidative stress inhibits the regenerative capacity of more mature hepatocytes.[11,12] Oxidative stress is thought to play a major role in the pathogenesis of both alcoholic and nonalcoholic fatty liver disease (NAFLD).[13,14] The replicative activity of mature hepatocytes is also known to be inhibited in patients with alcoholic hepatitis,[15] rodents with alcohol-induced fatty livers,[16] and in some animal models of NAFLD.[17,18] Although the combination of oxidative liver damage and inhibited hepatocyte proliferation provides a strong stimulus for oval cell accumulation in the liver, whether or not this cell population is expanded in fatty liver disease (FLD) has, to our knowledge, never been studied.

We therefore studied three different murine models of FLD [ie, genetically obese (ob/ob) mice and normal mice with fatty livers induced either by ethanol (EtOH) or methionine choline-deficient (MCD) diets], as well as patients with FLD related to either NAFLD or chronic alcohol abuse.

## Materials and Methods

### Murine Models of FLD

#### Animals

Adult (8 to 10 weeks of age) male C57BL-6 ob/ob mice, their lean littermates, and age- and gender-matched wild-type C57BL-6 were purchased from Jack-

Supported by research grants from the National Institutes of Health (RO1 AA010154 and RO1 DK3579 to A. M. D.) and F. W. O. Vlaanderen (G.0139.00N to T. R.).

Accepted for publication June 12, 2003.

Address reprint requests to Anna Mae Diehl, M.D., The Johns Hopkins University, 912 Ross Building, 720 Rutland St., Baltimore, Maryland 21205. E-mail: adiehl1@jhmi.edu.

son Laboratories (Bar Harbor, ME). Ob/ob mice and their lean littermates were fed standard chow. Wild-type mice were fed experimental diets: some ($n$ = 32) received liquid diets that contained 4% EtOH (v/v) (BioServ Inc., Frenchtown, NJ) for 4 weeks; others ($n$ = 32) were pair-fed the same volume of diet in which dextrin maltose was substituted isocalorically for EtOH; and still others were given methionine and choline-deficient diets (ICN diet catalog no. 96 0439, Costa Mesa, CA) ($n$ = 24) or methionine choline-sufficient diets ($n$ = 24) from the same manufacturer.

To induce hepatocyte proliferation, mice were subjected to 70% partial hepatectomy (PH) or treated with 1,4-bis[2-(3,5-dichloropyridyloxy)] benzene (TCPOBOP gift from Dr. A. Columbono, University of Cagliari, Cagliari, Italy) or ethionine, pharmacological agents that induce hepatocarcinogenesis.[19,20] PHs were performed under light ether anesthesia using the methods of Higgins and Andersen,[21] as we described.[22] Mice ($n$ = 4/group/time point) were sacrificed either immediately before PH or at various times (0.5, 1, 24, 36, or 48 hours) after PH. PH was performed on 20 ob/ob mice, 20 of their lean littermates, and 45 wild-type mice that were fed either EtOH (Sigma, St. Louis, MO) ($n$ = 25) or control ($n$ = 20) diets. Twelve other ob/ob mice and 12 of their lean littermates were gavaged with a single dose of TCPOBOP (6 mg/100 g body weight) or an equivalent volume of vehicle (corn oil) and sacrificed 4 days later because this protocol induces significant hepatocyte DNA synthesis and hepatomegaly in normal mice.[20] Finally, 24 chow-fed ob/ob mice and 24 mice that were fed either methionine choline-deficient diets ($n$ = 12 ob/ob mice and 12 lean controls) or the respective control diet ($n$ = 12 ob/ob mice and 12 lean mice) were given ethionine in their drinking water (final concentration, 0.15%) for 10 days to induce hepatic progenitor cell accumulation.[23] In all of the aforementioned studies, one liver sample from each mouse was fixed in buffered formalin and another sample was snap-frozen in liquid nitrogen-cooled isopentane and stored at −80°C.

### *Immunohistochemistry*

Four-$\mu$m-thick paraffin sections were deparaffinized and rehydrated, followed by heating in a microwave oven for 10 minutes at 750 W in citrate buffer, pH 6.0. Incubation with primary antibodies was performed at room temperature for 30 minutes. The polyclonal antibody against 56- and 64-kd human callus cytokeratins (dilution 1:200; DAKO, Glostrup, Denmark) was followed by undiluted anti-rabbit Envisiou (DAKO). Monoclonal mouse OV6 antibody (a kind gift from Stewart Sell, Albany Medical College, Albany, NY) was detected using the DAKO Animal Research Kit, peroxidase (DAKO). Oval cells (putative liver cell progenitors) were defined as small cells with an oval nucleus and little cytoplasm either singular or organized in arborizing ductular structures.[24] Strong reactivity for cytokeratins and oval cell marker OV-6 were used for the assessment of progenitor cells. The interlobular bile duct was defined as being a tubular structure with a recognizable lumen and associated with a branch of the hepatic artery. Before each counting in a portal tract, the interlobular bile duct was looked for and excluded for the countings. The number of oval cells was subsequently assessed in each biopsy, by calculating the average number of hepatic oval cells per high-power field (HPF) based on a count of oval cells in five nonoverlapping HPFs, using a ×40 objective.

### *Determination of Hepatic Mitochondrial Generation of Reactive Oxygen Species (ROS)*

Mitochondria were isolated from fresh liver samples obtained at the time of sacrifice.[7] Protein concentration was determined with the BSA assay (BioRad, Rockford, IL). Lucigenin (5 $\mu$mol/L bis *N*-methylacridinium; Sigma, Rockport, IL) was used to detect superoxide anion ($O_2^-$) and luminol (10 $\mu$mol/L 5-amino-2,3-dihydro-1,4-phthalazinedione, Sigma) was used to measure hydrogen peroxide ($H_2O_2$) generation. Briefly, mitochondria from an individual mouse were suspended in air-saturated reaction buffer (70 mmol/L sucrose, 220 mmol/L mannitol, 2 mmol/L Hepes, 2.5 m$\mu$mol/L $KH_2PO_4$, 2.5 mmol/L $MgCl_2$, 0.5 mmol/L ethylenediaminetetraacetic acid, and 0.1% bovine serum albumin, pH 7.4) plus substrate (6 mmol/L of succinate) (final concentration, 0.1 mg mitochondrial protein/ml) at 37°C. Each reaction was performed in triplicate. $O_2^-$ and $H_2O_2$ production by mitochondrial suspensions from six to eight mice/treatment group were evaluated by monitoring chemiluminescence continuously throughout a 60-minute period in a Berthold Biolumat LB9595 luminometer.[25]

### *Evaluation of ROS Regulatory Enzymes*

Mitochondrial preparations from the same mice were also assessed for the content of reduced glutathione (GSH) and the activities of several enzymes that regulate ROS production/detoxification. GSH content was assayed according to a modification of the protocol originally described by Hissin and Hilf[26] using reagents from Calbiochem Co. (San Diego, CA). Mitochondrial GSH content was calculated using a concurrently run standard curve. Mitochondrial superoxide dismutase (MnSOD) activity was measured in mitochondrial pellets (1 mg) by a modification of the assay described by Flohe and Otting[27] using Calbiochem reagents, including 5,6,6a,11b-tetrahydro-3,9,10-trihydroxybenzofluorene, which undergoes alkaline autoxidation in a MnSOD-catalyzed reaction that yields a chromophore that absorbs maximally at 525 nm. MnSOD activity was calculated using a concurrently run standard curve. Mitochondrial glutathione peroxidase (GPx) activity was measured using reagents from Calbiochem. Mitochondrial protein (50 $\mu$g) were suspended in 1 ml of buffer (50 mmol/L Tris-HCl, pH 7.6, 5 mmol/L ethylenediaminetetraacetic acid, 1 mmol/L GSH, 0.22 mmol/L NADPH, and 0.4 U of glutathione reductase) and *tert*-butyl hydroperoxide (final concentration, 0.22 mmol/L) was added to initiate NADPH consumption, which was monitored at 340 nm in a spectrophotometer. One nmol of NADPH consumed/min/ml = 1 mU/ml GPx activity.

## *Human Tissue Samples*

### *Patient Populations*

We retrospectively studied 45 liver biopsies obtained from the files from the Department of Pathology, University Hospital Leuven. Twenty patients were diagnosed with NAFLD on the basis of histology, a history of diabetes mellitus or obesity, no history of alcohol abuse, and no evidence of other causes of liver disease on serological testing. Twenty-five patients with alcoholic liver disease (ALD) were selected on the basis of histology, a clinical history of alcohol abuse, and no evidence of other causes of liver disease on serological testing. As a control group, archival normal liver tissue was obtained from three patients without histopathological, biochemical, or serological evidence of liver disease.

### *Histopathology Assessment and Immunohistochemistry*

For assessment of histopathology and fibrosis, the sections were routinely stained with hematoxylin and eosin, Hall's, Sirius Red, PAS after amylase digestion. The degree of fibrosis was scored according to the Brunt classification of fibrosis/cirrhosis.[28] We performed immunohistochemistry on B5-fixed, paraffin-embedded material, using monoclonal antibodies against cytokeratin 7, a known marker for hepatic oval cells and intermediate hepatocyte-like cells (HepLCs).[7] The number of progenitor cells was subsequently assessed in each biopsy, by calculating the average number of oval cells per HPF based on a count of oval cells in five nonoverlapping HPFs, using a ×40 objective. We used the same approach as in the mice models: the interlobular bile ducts were located and excluded from the countings, while ductules and single progenitor cells were counted as the ductular progenitor cell compartment.

More extensive phenotyping of the oval cells and their progeny was performed as previously described,[7] using antibodies against OV-6, cytokeratin (CK)-19, chromogranin-A (chrom-A), and neural cell adhesion marker on selected frozen biopsies of five NAFLD and five ALD patients. Cells were scored as oval cells or their progeny on the basis of morphological and immunohistochemical criteria.[7,24,29]

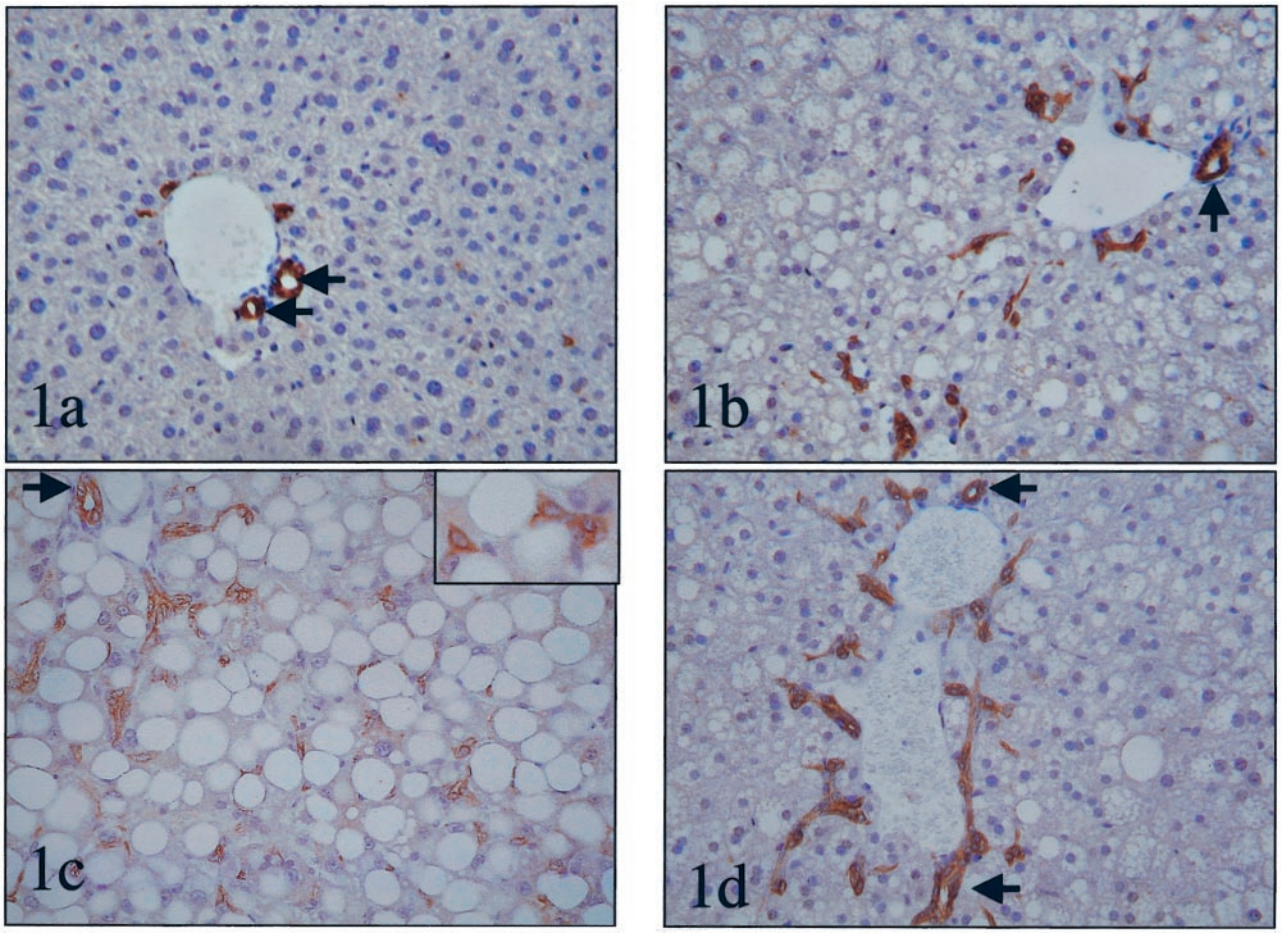


**Figure 1.** Oval cell accumulation in mice with fatty livers. Immunohistochemistry for bile duct-type cytokeratins was used to demonstrate oval cells in liver sections from healthy control mice (OV6 immunostain) (**a**) and mice with fatty livers caused by chronic EtOH consumption (OV6 immunostain) (**b**), feeding MCD diets (polyclonal cytokeratin stain). **Inset** shows detail of oval cells (**c**) or genetic obesity (ob/ob)(polyclonal cytokeratin stain) (**d**). Interlobular bile ducts (**small arrow**) were excluded from the countings, while the other immunoreactive cells were considered ductules/putative liver progenitor cells. Original magnifications: ×200; ×400 (**inset** in **c**).

**Table 1.** Mean Number of Progenitor Cells in Different Mouse Models

| Experimental group | OV-6 positive cells/ field |
|---|---|
| Control | 3 (1) |
| EtOH (4 weeks) | 32 (9) |
| Ob/ob | 23 (9) |
| Lean + partial hepatectomy | 9 (2) (at the peak) |
| EtOH + partial hepatectomy | 42 (8) (at the peak) |
| Ob/ob + partial hepatectomy | 38 (10) (at the peak) |
| Lean MCD (2 weeks) | 14 (4) |
| Lean ½ MCD + ethionine | 40 (8) |
| Ob/ob + ethionine | 170 (10) |
| Lean TCPOBOP | 36 (4) |
| Ob/ob + TCPOBOP | 63 (8) |

Results are mean (±SEM) per field with ×400 objective from control mice, EtOH-fed mice, ob/ob mice, MCD diet-fed mice, TCPOBOP-fed mice. EtOH, ethanol; MCD, methionine choline-deficient. EtOH-fed mice received liquid diets that contained 4% EtOH (vol/vol) for 4 weeks. Mice were fed MCD diets for 2 weeks. TCPOBOP was given in a single dose (6 mg/100 g body weight) and animals were sacrificed 4 days later.

At baseline, mice with fatty livers have significantly more OV-6+ (oval) cells than controls ($P < 0.001$ controls *versus* others). PH and tumor-promoting drugs generally increase the number of oval cells, but fatty livers always show twofold to fourfold more oval cells than similarly treated controls. Ethionine-treated ob/ob mice have the most oval cells.

$P < 0.001$ for ob/ob *versus* lean mice on control diets; $P < 0.005$ for lean mice on MCD diet *versus* lean mice on control chow; $P < 0.001$ for lean mice on one half MCD diet + ethionine compared to lean mice on MCD diet; $P < 0.001$ for ob/ob mice on control chow + ethionine *versus* lean mice on one half MCD diet + ethionine; $P < 0.001$ for ob/ob mice with TCPOBOP *versus* lean with TCPOBOP.

#### *Electron Microscopy*

Electron microscopy was performed on small liver fragments of four patients in the NAFLD group and six patients in the ALD group. The fragments were immediately fixed in 2.5% glutaraldehyde and 0.1 mol/L of phosphate buffer. After postfixation in 1% osmium tetroxide and 0.1 mol/L of phosphate buffer, the samples were dehydrated in graded series of alcohol and embedded in epoxy resin. Ultrathin sections were cut, stained with uranyl acetate and lead citrate, and examined using a Zeiss EM 10 electron microscope.

### *Statistical Analysis*

Analysis of variance was used to compare differences in Ov-6 (+) cell numbers, ROS production, ROS-regulatory enzyme activities, and GSH content among the various groups of mice. The significance of the correlation between the oval cell/HepLC count and the extent of fibrosis was assessed using the Kruskal-Wallis test. The Wilcoxon-Mann Whitney test was used to determine whether the difference in grade of activation of oval cells and HepLCs between ALD and NAFLD was significant. Significance was accepted for $P$ values $<0.05$.

**Table 2.** GSH Content and Activities of ROS-regulatory Enzymes in Hepatic Mitochondria from Different Mouse Models of Fatty Liver Disease

| | GSH ($\mu$g/mg protein) | MnSOD (U/mg protein) | GPx (U/mg protein) |
|---|---|---|---|
| Control | 16 (0.2) | 1,991 (87) | 3.6 (0.02) |
| EtOH-fed | 10 (0.7)* | 3,273 (547)† | 8.5 (0.3)‡ |
| Ob/ob | 18 (1.0)* | 2,396 (109)† | 3.2 (0.3)‡ |
| MCD-diet | 23 (2.0)* | 2,401 (251)† | 5.7 (0.4)‡ |

Results are mean (±SEM) for each group (six mice/group). GSH, reduced glutathione; MnSOD, manganese superoxide dismutase; GPx, glutathione peroxidase. GSH content and enzyme activities were evaluated as described in Materials and Methods.

*$P < 0.05$ for GSH in experimental model *versus* control.

†$P < 0.05$ for MnSOD in experimental model *versus* control.

‡$P < 0.05$ for GPx in experimental model *versus* control.

## *Results*

### *Studies of Mice with Fatty Livers*

#### *Oval Cell Accumulation*

In the absence of any added stimulus for liver regeneration, the numbers of oval cells were significantly increased in all three groups with fatty livers (Figure 1, Table 1).

#### *Mechanisms for Progenitor Cell Accumulation*

Various pharmacological agents that cause oxidative stress inhibit DNA synthesis in mature hepatocytes and induce compensatory mechanisms, including the recruitment of hepatic progenitors.[19,23] In view of reports that FLD inhibits replication of mature hepatocytes[17,18] and our new evidence for oval cell accumulation in hepatic steatosis, we postulated that oxidative stress would be a common feature of the various murine models of FLD. We therefore assessed the activities of various enzymes that regulate ROS generation, glutathione (GSH) content, and $O_2^-$ and $H_2O_2$ production in fatty liver and control liver mitochondria. Compared to control mitochondria, fatty liver mitochondria uniformly demonstrated alterations in ROS-regulatory enzymes and/or GSH content that favor excessive ROS production (Table 2). For example, the activity of manganese superoxide dismutase (MnSOD), the enzyme that converts $O_2^-$ to $H_2O_2$, is increased in all three groups with fatty livers. This is compounded by reduced activity of glutathione peroxidase (GPx) in ob/ob mitochondria and decreased mitochondrial GSH content in mitochondria from EtOH-fed mice. As predicted, mitochondrial ROS production is increased significantly in all three types of fatty liver, although the relative contributions of $O_2^-$ and $H_2O_2$ to this process appear to vary among the different models (Table 3). For example, mitochondria from MCD diet-fed mice exhibit the greatest production of $O_2^-$, whereas those obtained from ob/ob mice produce the highest levels of $H_2O_2$. Compared to the other two groups with fatty livers, mitochondria from EtOH-fed mice produce intermediate levels of both $O_2^-$ and $H_2O_2$. Whether or not these differences in the types of ROS that predominate in various models of FLD have biological significance is unknown. However, this merits consideration because greater numbers of oval cells were observed in EtOH-fed and ob/ob mice, which produced higher levels of $H_2O_2$ than MCD diet-fed mice, which produced relatively little $H_2O_2$ despite generating the highest levels of $O_2^-$ (Figure 1, Table 1).

**Table 3.** Hepatic Mitochondrial Production of ROS in Different Mouse Models of Fatty Liver Disease

| | $O_2^-$ (integrated counts × $10^6$) | $H_2O_2$ (integrated counts × $10^6$) | *P* value |
|---|---|---|---|
| Control | 28 (2) | 26 (0.5) | — |
| EtOH-fed | 32 (1)* | 43 (6)† | <0.05,* <0.01† |
| Ob/ob | 24 (1)* | 69 (9)† | <0.05,* <0.001† |
| MCD diet | 39 (4)* | 28 (0.3)† | <0.001,* <0.05† |

Results are mean (±SEM) from six control mice, six EtOH-fed mice, six ob/ob mice, and six MCD diet-fed mice. EtOH, ethanol; MCD, methionine choline-deficient. EtOH-fed mice received liquid diets that contained 4% EtOH (vol/vol) for 4 weeks. Mice were fed MCD diets for 2 weeks. Hepatic mitochondria were isolated from each mouse and ROS production was evaluated as described in Materials and Methods. $O_2^-$ production, area under the curve for lucigenin-derived chemiluminescence; $H_2O_2$ production, area under the curve for luminol-derived chemiluminescence.

**P* value for production of $O_2^-$ by experimental model *versus* control mice.

†*P* value for production of $H_2O_2$ by experimental model *versus* control mice.

### *Progenitor Cell Accumulation and Liver Regeneration*

Progenitor cell activation has mainly been reported in rat models associated with inhibited proliferation of mature hepatocytes. By monitoring hepatocyte expression of proliferating cell nuclear antigen and incorporation of BrdU, we recently showed that replication of mature hepatocytes is severely impaired after PH in mice with obesity-related[18] or alcohol-induced[30] FLD, compared to their respective healthy controls. Here, we studied liver samples from these same mice to determine whether inhibited hepatocyte replication was accompanied by the hepatic accumulation of oval cells after PH. As shown in Figure 2a, slight variations in the numbers of oval cells occur in normal mice after PH, with a small (but highly significant, $P < 0.0005$) increase in oval cell accumulation occurring at ~36 hours, the time period when hepatocyte DNA synthesis typically becomes maximal in healthy livers. Before PH, significantly greater numbers of Ov-6 (+) cells are demonstrated in both fatty liver models (ie, EtOH-fed and ob/ob mice) ($P < 0.0001$ for mice with fatty livers *versus* control mice at time 0). In addition, wide fluctuations in the size of the putative progenitor cell population occur after PH. By 36 hours after PH the numbers of oval cells in the fatty liver remnants have increased by ~70%, leading to a significant increase in the size of this cellular population compared to pre-PH values ($P < 0.01$ at 36 hours compared to time 0). Moreover, by 36 to 48 hours after PH, in addition to single oval

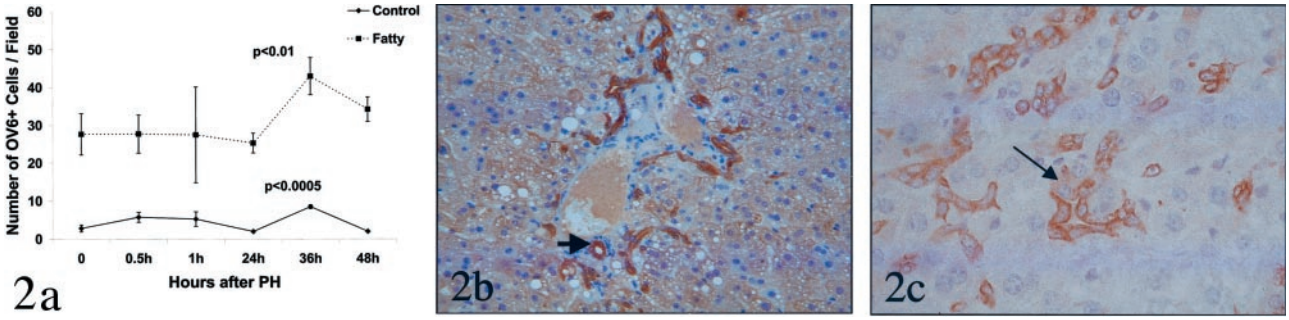


**Figure 2.** Accumulation of putative liver progenitor cells in liver remnants after PH. **a:** Immunohistochemistry was used to demonstrate OV6 (+) cells in liver sections from two groups of healthy control mice (lean littermates of ob/ob mice, $n = 12$; wild-type mice pair-fed so that caloric intake matched EtOH-fed mice, $n = 12$) and two groups of mice with fatty livers (ob/ob mice, $n = 12$; EtOH-fed mice, $n = 12$) at various time points after PH. Because results in both control groups were similar, data are pooled and shown as the control line on this graph ($n = 4$ mice/time point). Similarly, there were no significant differences between ob/ob mice and EtOH-fed mice, so these results are pooled and results are shown as the fatty line on this graph ($n = 4$ mice/time point). *, $P < 0.0005$ *versus* control at time 0; #, $P < 0.01$ for fatty at time 0. **b:** Photomicrograph of Ov-6 (+) cells in a representative mouse with fatty liver at 36 hours after PH. In addition to cords of small oval cells, numerous intermediate hepatocyte-like cells showing a submembranous staining pattern for Ov-6 can be seen. **c:** High-magnification photomicrograph of CK7 (+) cells in another representative mouse with fatty liver at 48 hours after PH. Note the appearance of a small hepatocyte-like cell (**arrow**). This cell is immediately adjacent to cords of small oval cells. Cytokeratin 7 stain; original magnification, ×400 (**c**).

**Table 4.** Hepatic Effects of TCPOBOP

| | Lean | ob/ob |
|---|---|---|
| Hepatocyte BrdU incorporation (fold greater than vehicle-treated control) | 16 (3)* | 1.3 (0.1) |
| Hepatocyte mitoses (no. mitoses/50 HPF) | 155 (69)* | 7 (10) |
| Hepatocyte polyploidy (fold greater than vehicle-treated control) | 2.7 (0.3)* | 1.3 (0.2) |
| Liver Weight (fold greater than vehicle-treated control) | 1.5 (0.2)† | 1.4 (0.2)† |

Mean (±SEM) results of six lean and five ob/ob mice 4 days after TCPOBOP *versus* six lean control and six ob/ob control mice 4 days after vehicle (corn oil). One ob/ob mouse died 24 hours after TCPOBOP. HPF, high power field (×200 magnification). Hepatocyte BrdU incorporation and mitoses were assessed by counting BrdU+ hepatocyte nuclei or mitotic figures in 50 randomly selected fields on coded sections from each mouse. No mitotic figures were noted in vehicle-treated controls from either group. Hepatocyte polyploidy (DNA content > 4n) were evaluated by flow cytometry of propidium iodide-stained liver nuclei isolated from a frozen liver sample from each mouse.

**P* < 0.01 *versus* vehicle treated, lean controls and versus TCPOBOP-treated ob/ob group.

†*P* < 0.05 *versus* respective, vehicle-treated control for each group.

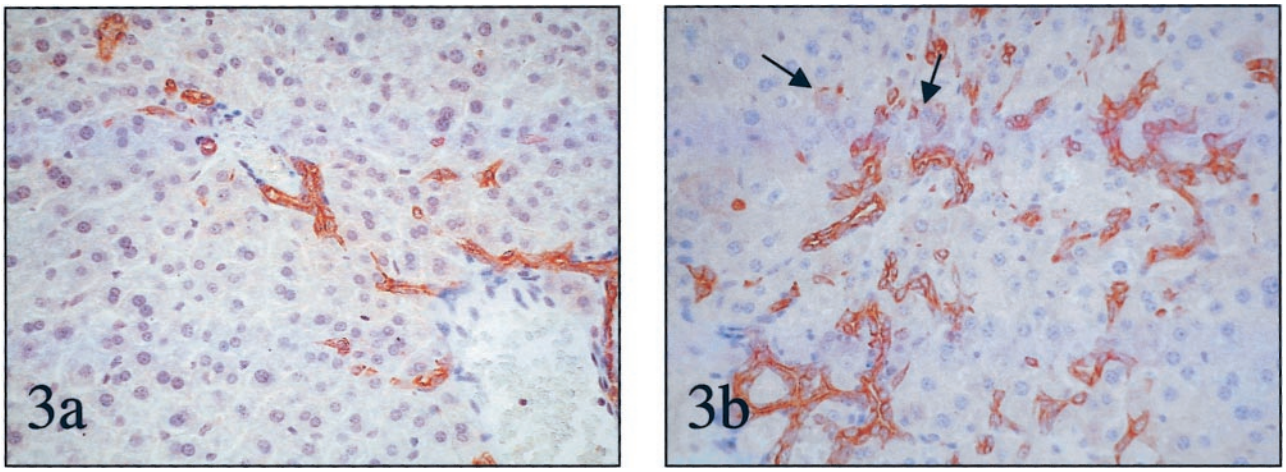


**Figure 3.** Accumulation of putative liver progenitor cells after treatment with the tumor-promoting drug, ethionine. **a:** Oval cells in the liver of a representative lean mouse fed one-half MCD diet plus ethionine. **b:** Oval cells in the liver of a representative ob/ob mouse fed control chow plus ethionine. Note intermediate hepatocyte-like cells (**arrows**). mOV-6 staining; original magnifications, ×200.

cells and strands of oval cells, intermediate hepatocyte-like cells, in continuity with oval cells, are abundant in the fatty livers, but not in controls. These intermediate hepatocyte-like cells are larger and show a submembranous cytokeratin-staining pattern, instead of the cytoplasmic staining pattern of small oval cells (Figure 2, b and c). This finding suggests that oval cell differentiation may contribute to the regeneration of fatty livers after PH.

To determine whether or not the oval cell response was specific to liver regeneration induced by PH, we treated ob/ob mice and their lean littermates with TCPOBOP, a tumor-promoting agent that is known to increase hepatocyte turnover in normal rodents.[20] After TCPOBOP treatment, hepatocyte DNA synthesis and proliferation were significantly greater in lean mice than in ob/ob mice. Nevertheless, similar degrees of hepatomegaly developed in the two groups (Table 4). Compared to PH (which does not cause hepatocellular carcinoma in normal mice), TCPOBOP treatment was followed by significantly greater accumulation of oval cells in both lean and ob/ob mice. As noted after PH, after TCPOBOP treatment, the numbers of oval cells in mice with fatty livers were significantly greater than controls (Table 1). Thus, in ob/ob mice that exhibit chronic oxidative stress and inhibited replication of mature hepatocytes after either PH or toxic liver injury, the ensuing regenerative responses are characterized by increased hepatic accumulation of putative progenitor cells.

Although the present study provides novel evidence for oval cell expansion by the hepatic carcinogen, TCPOBOP, oval cells are widely acknowledged to play a role in hepatocarcinogenesis after exposure to ethionine.[19] Feeding MCD diets to induce oxidative stress amplifies ethionine-related expansion of hepatic oval cell populations in normal mice.[23] Given that we observed increased ROS production and profound inhibition of mature hepatocyte proliferation in ob/ob mice,[18] we postulated that ethionine would induce oval cell accumulation in ob/ob livers, even when these mice are fed normal chow.

As others have shown, ethionine expanded the oval cell population in lean control mice that were fed antioxidant-depleted diets (Table 1). However, the drug dramatically increased the hepatic accumulation of Ov-6 (+) cells in chow-fed ob/ob mice. In fact, the numbers of Ov-6 (+) cells in the livers of ethionine treated, chow-fed ob/ob mice significantly exceeded the numbers of these cells in the livers of one-half MCD plus ethionine-treated wild-type mice (Table 1 and Figure 3, a and b).

**Figure 4.** Accumulation of putative liver progenitor cells in patients with NAFLD and AFLD. Representative photomicrographs from human samples with ALD (**a–d**) and NAFLD (**e–f**). **a:** Paraffin section of a cirrhotic stage of ALD (Brunt stage 4) immunostained for cytokeratin 7, showing single small oval cells (**small arrows**), extending far into the parenchyma. Intermediate hepatocyte-like cells (**open arrows**) are present, often in continuity with oval cells. These cells are numerous in the cirrhotic stage of ALD, suggesting more differentiation toward hepatocytes in this stage of the disease. **b:** Frozen section of ALD Brunt stage 4 (cirrhotic liver) immunostained for cytokeratin 19, showing reactive ductules (**large arrow**) and oval cells (**small arrows**). Intermediate hepatocyte-like cells are not reactive for cytokeratin 19. **c** and **d:** Frozen section of ALD Brunt stage 4 (cirrhotic liver) immunostained for Ov-6 (**c**) and chromogranin-A (**d**), showing a strikingly high number of intermediate hepatocyte-like cells, suggesting a high degree of differentiation of oval cells toward hepatocytes in the cirrhotic stage of the disease. Cytokeratin 7, OV6, and chromogranin-A are immunoreactive in intermediate cells, while cytokeratin 19 is not or hardly; such as we have previously shown, cytokeratin 19 is a marker that is lost early during differentiation from oval cells toward hepatocytes. P, portal tract. **e:** Paraffin section of NAFLD Brunt stage 2, immunostained for cytokeratin 7, showing the putative progenitor cells, extending into the steatotic parenchyma. In this stage, no intermediate hepatocyte-like cells are seen. **f:** Frozen section of NAFLD Brunt stage 3, immunostained for cytokeratin 19, showing single progenitor cells (**small arrows**) and reactive ductules. **g:** Frozen section of NAFLD Brunt stage 3, immunostained for Ov-6. Oval cells (**small arrows**) and intermediate hepatocyte-like cells (**open arrow**) are present. Note that intermediate hepatocytes are less numerous compared to the cirrhotic stage of ALD (shown in **c**). **h:** Frozen section of NAFLD Brunt stage 3, immunostained for chromogranin-A, showing putative progenitor cells (**small arrows**) and intermediate hepatocyte-like cells (**open arrow**), which are less numerous compared to the cirrhotic stage of ALD (shown in **d**). Original magnifications, ×160.

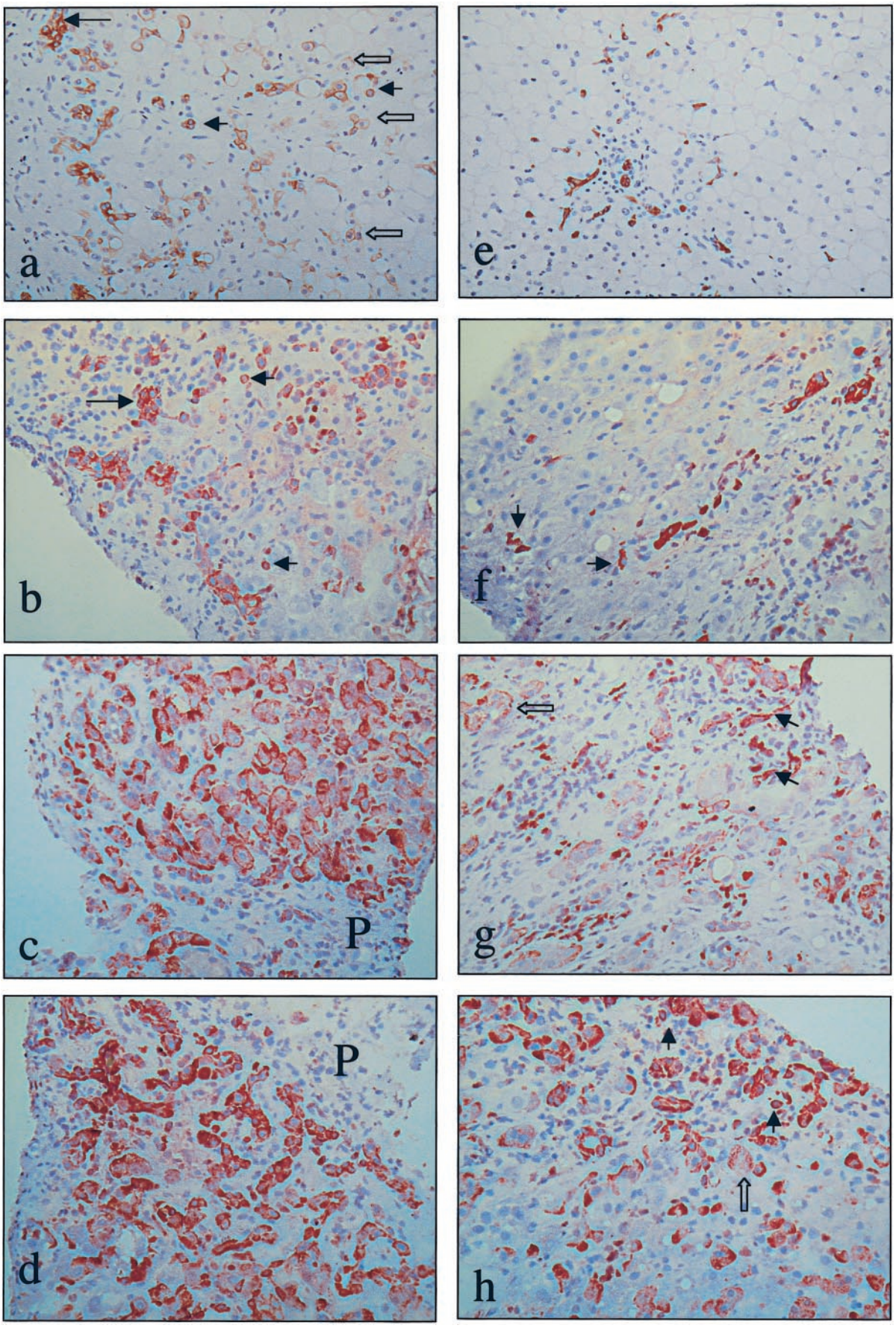
a
e
b
f
c
P
g
P
d
h

**Table 5.** Accumulation of Putative Progenitor Cells According to Fibrosis Stage in Patients with NAFLD and ALD

| Fibrosis grade | Mean oval cells NAFLD and ALD | Mean intermediate hepatocytes NAFLD and ALD | NAFLD oval cells | NAFLD intermediate hepatocyte-like cells | ALD oval cells | ALD intermediate hepatocyte-like cells |
|---|---|---|---|---|---|---|
| 0 | 13.5 (5.9) | 0.8 (1.5) | 15.8 (4.5) | 1.5 (2.1) | 11.1 (7.7) | 0.1 (0.1) |
| 1 | 20.3 (22.6) | 0.9 (1.4) | 13.6 | 3 | 22.5 (27.1)* | 0.2 (0.3) |
| 2 | 18 (14.4) | 2.8 (4.7) | 14.3 (6.6) | 1.3 (1.9) | 29.1 (26.7)* | 7.2 (8.2)* |
| 3 | 32 (26.4)* | 24.8 (32.5)* | 11.2 (3.9) | 1.4 (0.2) | 38.3 (26.9)* | 30.6 (34.1)* |
| 4 | 92.9 (34.1)* | 46 (22.4)* | 150.2* | 21.6 (8.4)* | 86 (29)* | 48.7 (22)* |

Immunohistochemistry was used to demonstrate putative progenitor cells in human liver biopsies. The numbers of oval cells and intermediate hepatocytes were counted in five fields under ×400 magnification. Results are mean (SD) data from patients at each stage of the disease.
*$P < 0.05$ *versus* stage 0 (no fibrosis) for the same disease.

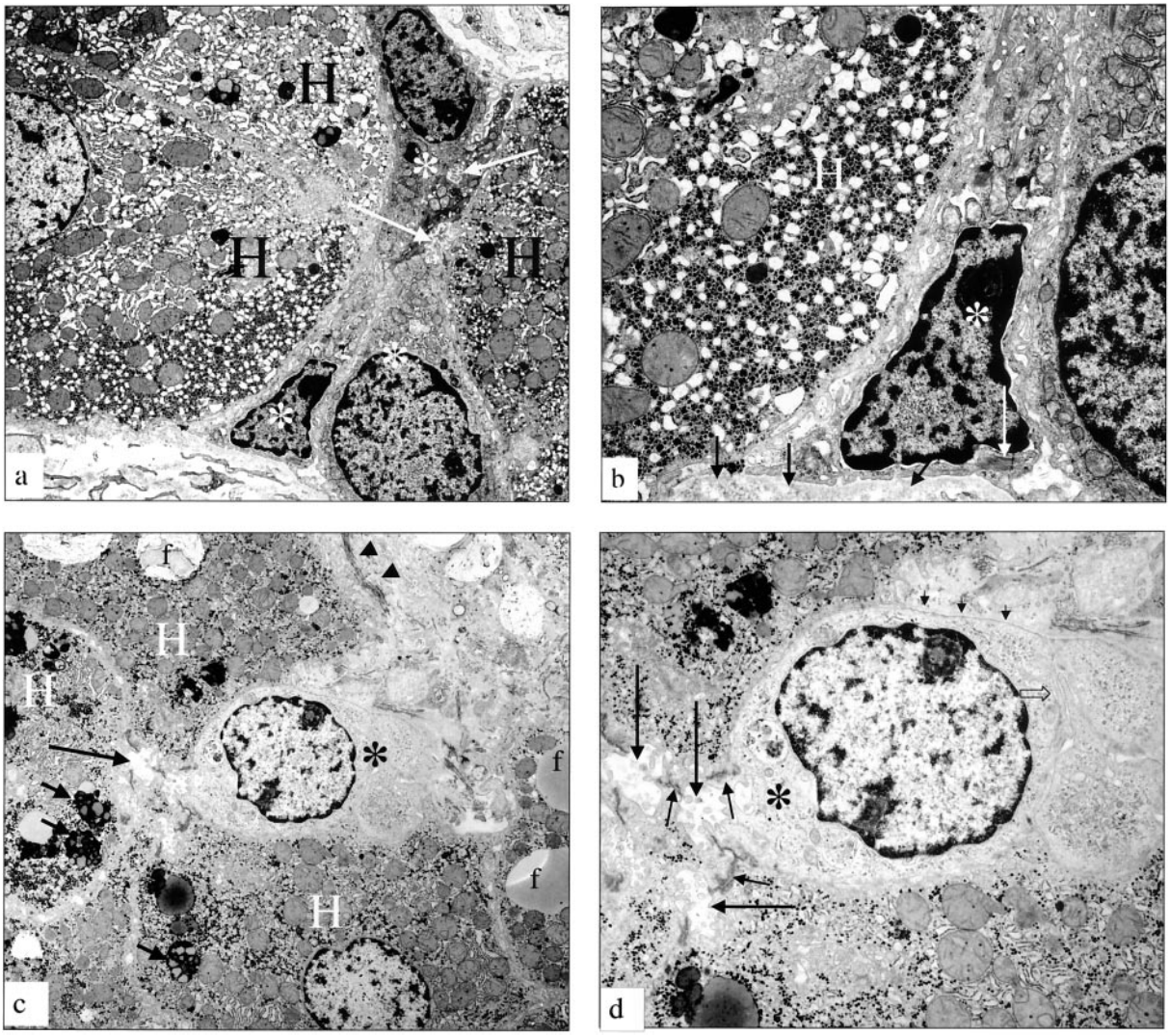


**Figure 5.** Electron micrographs of putative progenitor cells in patients with FLD. **a:** Electron micrograph of a liver biopsy from a patient with ALD (active cirrhosis). A group of small epithelial hepatic progenitor cells (**white asterisk**) are arranged between hepatocytes (H). These cells range from very immature (**a**, **bottom**) to somewhat differentiating toward the hepatocyte lineage. The small cells form a hemicanaliculus (**arrow**) with the neighboring hepatocytes, showing that the differentiation direction is toward hepatocytes. **b:** Electron micrograph of a liver biopsy from a patient with ALD (active cirrhosis). Higher magnification of the most immature hepatic progenitor cell (**asterisk**) shown in **a**. H, adjacent hepatocyte. Bundles of tonofilaments (**long white arrow**) are seen in the cytoplasm; these tonofilaments distinguish these cells from nonepithelial cells such as endothelial cells or Kupffer cells; the cell rests on a basement membrane (**short arrows**). **c:** Electron micrograph of a liver from a patient with NAFLD. A small epithelial hepatic progenitor cell (**asterisk**) is wedged in between hepatocytes (H). Note fat droplets (f) and lipofuscin granules (**small arrows**). Collagen bundles are present in Disse's space (**arrowheads**). **d:** Electron micrograph of a liver from a patient with NAFLD showing a higher magnification of the same progenitor cell (**asterisk**) from **c**. A tortuous bile canaliculus (**large arrow**) sealed by junctional complexes of the desmosomal type, typical for epithelial cells (**small arrows**) is seen between two hepatocytes (H) and the progenitor cell (**asterisk**). Note the basement membrane (**short arrows**) and villous interdigitations (**open arrow**) with neighboring progenitor cell, which are features of the biliary lineage. Original magnifications: ×7150 (**a**, **c**); ×18,400 (**b**); ×14,500 (**d**).

## *Studies of Patients with NAFLD and ALD*

### *Immunohistochemistry*

Progenitor cells resembling oval cells were rarely detected in the normal controls. However, in patients with NAFLD and in those with ALD, we consistently noted small single oval cells (CK7, CK19, Ov-6, chromogranin-A+ cells). These cells were located in the periportal area, and often extended into the parenchyma of the lobule. Reactive ductules (CK7, CK19, Ov-6, chromogranin-A, neural cell adhesion marker + structures) were also seen at the portal-parenchymal interface. Because bile ductules harbor the progenitor cells in the canal of Hering, we considered the whole of reactive ductules and single oval cells the expanded progenitor cell compartment. Intermediate hepatocyte-like cells (HepLCs) that express CK7, chromogranin-A, and OV-6, were seen in continuity with the oval cells (Figure 4)

In ALD, the number of oval cells/ductules and the number of HepLCs correlated strongly with the degree of fibrosis ($P < 0.05$). With increasing fibrosis stage, similar increases in oval cells and HepLPCs were noted in both groups (Table 5). Thus, putative hepatic progenitor cells accumulate in the livers of patients with FLD. Also, as we have demonstrated in patients with chronic viral hepatitis,[9] in both ALD and NAFLD patients, the numbers of putative hepatic progenitors increases with the severity of the underlying liver disease.[31]

### *Electron Microscopy*

The overall ultrastructural features of the liver parenchyma of NAFLD patients and ALD patients were similar and comparable to those described in the literature.[32] Of note, mitochondrial variations in sizes and shape, as well as rearrangement of cristae and paracrystalline inclusions were seen in both the NAFLD and the ALD biopsies, and there were no significant differences in the extent of mitochondrial pathology between the two groups. In all liver biopsies of NAFLD patients, small- to intermediate-sized progenitor cells, with epithelial characteristics, were identified in the periportal area (Figure 5). These small cells were found immediately adjacent to, or wedged between, hepatocytes. The hepatocytes adjacent to the small- to intermediate-sized cells typically exhibited abnormal mitochondrial morphology. The small cells themselves had an oval or round small nucleus, and a round nucleolus was typically noted at the nuclear margin. The cytoplasm contained a full assortment of organelles, and several bundles of tonofilaments were always obvious. These small cells are clearly different from endothelial and Kupffer cells. Endothelial cells, lined along the sinusoidal wall, are flattened and elongated cells with thin cytoplasmic processes, provided with fenestrae arranged in so-called sieve plates. A characteristic of these cells is the presence of pinocytotic pits and vesicles interfacing with a complex system of vacuoles, coated vesicles, and tubules. No tonofilaments are present. Kupffer cells are rather large star-shaped cells anchoring to the endothelial wall and bulging into the sinusoidal lumen. They are provided with numerous irregular microvilli and pseudopodia; their peripheral cell membrane contains numerous pinocytotic, phagocytic, and worm-like structures. In their rather voluminous cytoplasm many heterozygous lysosomes of different sizes are apparent. No tonofilaments are seen. Therefore, ultrastructural criteria clearly distinguish the small epithelial progenitor cells from other types of liver cells. In addition, in our tissue samples a basement membrane surrounded the sinusoidal pole of the small cells and early or well-formed junctional complexes of the desmosomal type joined them with adjacent hepatocytes. More voluminous small epithelial cells with a round nucleus were also noted, often forming a hemicanaliculus with neighboring hepatocytes. Fully developed junctional complexes joined these cells to hepatocytes.

The same small epithelial cells were obvious in the periportal parenchyma in the liver biopsies of patients with ALD, and biopsies from both groups exhibited a comparable number of these cells. In addition, tubular transformation of the liver plates was noted in some areas of biopsies from the two ALD patients who had active cirrhosis. In these locations, the numbers of progenitor cells were increased in comparison with noncirrhotic NAFLD and ALD biopsies. The tubular arrangements of hepatocytes and associated progenitor cells were surrounded by thick bundles of collagen. In contrast to the severe ultrastructural damage noted in most parenchymal hepatocytes, the tubularly arranged hepatocytes that were in continuity with progenitor cells usually displayed a normal ultrastructure.

## *Discussion*

Rat models of impaired hepatocyte replication show oxidative stress and activation of the liver progenitor cell compartment. Since we showed recently that mouse models of FLD have impaired hepatocyte replication, we studied different murine models of FLD and patients with NAFLD and ALD to determine whether progenitor cells increase in FLD and to clarify mechanisms that might mediate this response. In the present study, we demonstrate that ROS production by liver mitochondria is increased significantly in alcohol-fed mice, mice with diet-induced steatohepatitis, and genetically obese mice with FLD. In particular, all models exhibit excessive production of $H_2O_2$, a molecule that is known to induce potent cell-cycle inhibitors, such as p21.[33] We reported recently that p21 is up-regulated in both alcohol-fed mice and in obese ob/ob mice after PH and showed that PH induction of DNA synthesis by mature hepatocytes is impaired significantly in both mouse models.[30,34] Thus, the present evidence for increased $H_2O_2$ production by hepatocytes in various animal models of FLD suggests a general mechanism for inhibited replication of mature hepatocytes during chronic oxidative stress. The present study also extends our previous work by demonstrating that DNA synthesis in fatty hepatocytes is not merely inhibited after liver resection, but is also inhibited after exposure to TCPOBOP, a hepatotoxin and potent tumor promoter.[20]

Crary and Albrecht[15] have reported that hepatocyte expression of p21 is increased in liver biopsies from patients with ALD who exhibit impaired hepatocyte proliferation. These findings suggest that, as in various mouse models of FLD, increased hepatic oxidant stress promotes replicative senescence in mature human hepatocytes.

In addition, we show that ROS-related replicative senescence in mature hepatocytes is accompanied by expansion of oval cells (a putative liver progenitor cell population) in both mice and humans with FLD. Both in the murine models and in humans, no significant difference in the degree of progenitor cell activation was noted between NAFLD and ALD. This indicates that, similar to oxidant-induced replicative senescence, the progenitor cell response is somewhat stereotypical, ie, not related to a specific type of toxin or injury. These results are in good agreement with our previous findings of human progenitor cell activation across various degrees of chronic hepatitis, as well as in various etiologies of necrotizing hepatitis (toxic, viral, or autoimmune).[9,7,35] Taken together, these observations support the concept that oval cell expansion is a component of the liver's adaptive response to oxidative stress.

In humans, the degree of oval cell activation showed a positive correlation with the degree of fibrosis, a marker of liver disease chronicity ($P = 0.0017$). Moreover, the number of intermediate hepatocyte-like cells increased with the stage of the liver disease ($P = 0.0077$), suggesting cumulative hepatocyte loss promotes not only oval cell accumulation, but also the differentiation of oval cells toward hepatocytes. For example, the number of oval cells and HepLC was most impressive, both immunohistochemically and ultrastructurally, in the ALD patients who had progressed to cirrhosis. The ultrastructural appearance of the intermediate hepatocytes in cirrhotic liver was so strikingly normal (ie, undamaged) that this highly suggests that they originate from the putative progenitor cells. In noncirrhotic mice with obesity or alcohol-induced fatty livers, intermediate hepatocyte-like cells were recognizable at 36 and 48 hours after PH, and after ethionine treatment, consistent with the human evidence that a reduced mass of functional, mature hepatocytes (rather than cirrhosis per se) triggers the differentiation of oval cells toward hepatocytes. Interesting in this regard is our recent evidence that the expression of ATP-binding cassette proteins MRP-1, MRP-3, and MDR-1 is increased in the progenitor cell compartment in various human liver diseases.[36] These transporters are known to be cytoprotective. For example, MRP-1 helps cells to secrete GSSG or the GSH conjugates of 4-hydroxynononeal, products of oxidative stress reactions.[37] Therefore, the phenotype of oval cells may convey a survival advantage that permits them to accumulate in conditions that severely damage more mature hepatocytes. This, in turn, helps to explain the positive relationship between oval cell and HepLC accumulation and reductions in mature hepatocyte mass: oxidant stress reduces the viability and expansion of mature hepatocytes, while sparing less mature hepatic progenitors. A similar paradigm has been implicated during neoplastic transformation.[3] Thus, it is tempting to speculate that hepatocellular carcinoma develops because chronic oxidative stress exerts a selection pressure that favors the outgrowth of progenitor cell clones that are most resistant to oxidant damage. Further studies are needed to evaluate this possibility. Fortunately, the present work proves that there are good small animal models for human FLD. These can be used to unravel the pathogenic mechanisms for FLD progression, including the evolution of hepatocellular carcinoma.

## References

1. Thorgeirsson SS, Factor VM, Snyderwine EG: Transgenic mouse models in carcinogenesis research and testing. Toxicol Lett 2000, 112–113:553–555
2. Evarts RP, Nagy P, Marsden E, Thorgeirsson SS: A precursor-product relationship exists between oval cells and hepatocytes in rat liver. Carcinogenesis 1987, 8:1737–1740
3. Sell S, Dunsford HA: Evidence for the stem cell origin of hepatocellular carcinoma and cholangiocarcinoma. Am J Pathol 1989, 134: 1347–1363
4. Libbrecht L, Meerman L, Kuipers F, Roskams T, Desmet V, Jansen P: Liver pathology and hepatocarcinogenesis in a long-term mouse model of erythropoietic protoporphyria. J Pathol 2003, 199:191–200
5. Hsia CC, Evarts RP, Nakatsukasa H, Marsden ER, Thorgeirsson SS: Occurrence of oval-type cells in hepatitis B virus-associated human hepatocarcinogenesis. Hepatology 1992, 16:1327–1333
6. Ruck P, Xiao JC, Pietsch T, Von Schweinitz D, Kaiserling E: Hepatic stem-like cells in hepatoblastoma: expression of cytokeratin 7, albumin and oval cell associated antigens detected by OV-1 and OV-6. Histopathology 1997, 31:324–329
7. Roskams T, De Vos R, Van Eyken P, Myazaki H, Van Damme B, Desmet V: Hepatic OV-6 expression in human liver disease and rat experiments: evidence for hepatic progenitor cells in man. J Hepatol 1998, 29:455–463
8. Crosby HA, Hubscher S, Fabris L, Joplin R, Sell S, Kelly D, Strain AJ: Immunocalization of putative human liver progenitor cells in livers from patients with end-stage primary biliary cirrhosis and sclerosing cholangitis using the monoclonal antibody OV-6. Am J Pathol 1998, 152:771–779
9. Libbrecht L, Desmet V, Van Damme B, Roskams T: Deep intralobular extension of human hepatic 'progenitor cells' correlates with parenchymal inflammation in chronic viral hepatitis: can 'progenitor cells' migrate? J Pathol 2000, 192:373–378
10. Libbrecht L, Desmet V, Van Damme B, Roskams T: The immunohistochemical phenotype of dysplastic foci in human liver: correlation with putative progenitor cells. J Hepatol 2000, 33:76–84
11. Ohlson LC, Koroxenidou L, Hallstrom IP: Inhibition of in vivo rat liver regeneration by 2-acetylaminofluorene affects the regulation of cell cycle-related proteins. Hepatology 1998, 27:691–696
12. Lindeman B, Skarpen E, Oksvold MP, Huitfeldt HS: The carcinogen 2-acetylaminofluorene inhibits activation and nuclear accumulation of cyclin-dependent kinase 2 in growth-induced rat liver. Mol Carcinog 2000, 27:190–199
13. Mehta K, Van Thiel DH, Shah N, Mobarhan S: Nonalcoholic fatty liver disease: pathogenesis and the role of antioxidants. Nutr Rev 2002, 60:289–293
14. Tsukamoto H, Lu SC: Current concepts in the pathogenesis of alcoholic liver injury. FASEB J 2001, 15:1335–1349
15. Crary GS, Albrecht JH: Expression of cyclin-dependent kinase inhibitor p21 in human liver. Hepatology 1998, 28:738–743
16. Wands JR, Carter EA, Bucher NL, Isselbacher KJ: Inhibition of hepatic regeneration in rats by acute and chronic ethanol intoxication. Gastroenterology 1979, 77:528–531
17. Selzner M, Clavien PA: Failure of regeneration of the steatotic rat liver: disruption at two different levels in the regeneration pathway. Hepatology 2000, 31:35–42
18. Yang SQ, Lin HZ, Mandal AK, Huang J, Diehl AM: Disrupted signaling and inhibited regeneration in obese mice with fatty livers: implications

for nonalcoholic fatty liver disease pathophysiology. Hepatology 2001, 34:694–706
19. Tarsetti F, Lenzi R, Salvi R, Schuler E, Rijhsinghani K, Lenzen R, Tavoloni N: Liver carcinogenesis associated with feeding of ethionine in a choline-free diet: evidence against a role of oval cells in the emergence of hepatocellular carcinoma. Hepatology 1993, 18:596–603
20. Dragani TA, Manenti G, Galliani G, Della Porta G: Promoting effects of 1,4-bis[2-(3,5-dichloropyridyloxy)]benzene in mouse hepatocarcinogenesis. Carcinogenesis 1985, 6:225–228
21. Higgins G, Andersen R: Experimental pathology of liver: restoration of liver of white rat following partial surgical removal. Arch Pathol 1931, 12:186–202
22. Lee FY, Li Y, Zhu H, Yang S, Lin HZ, Trush M, Diehl AM: Tumor necrosis factor increases mitochondrial oxidant production and induces expression of uncoupling protein-2 in the regenerating mice [correction of rat] liver. Hepatology 1999, 29:677–687
23. Akhurst B, Croager EJ, Farley-Roche CA, Ong JK, Dumble ML, Knight B, Yeoh GC: A modified choline-deficient, ethionine-supplemented diet protocol effectively induces oval cells in mouse liver. Hepatology 2001, 34:519–522
24. Sell S: Comparison of liver progenitor cells in human atypical ductular reactions with those seen in experimental models of liver injury. Hepatology 1998, 27:317–331
25. Yang S, Zhu H, Li Y, Lin H, Gabrielson K, Trush MA, Diehl AM: Mitochondrial adaptations to obesity-related oxidant stress. Arch Biochem Biophys 2000, 378:259–268
26. Hissin PJ, Hilf R: A fluorometric method for determination of oxidized and reduced glutathione in tissues. Anal Biochem 1976, 74:214–226
27. Flohe L, Otting F: Superoxide dismutase assays. Methods Enzymol 1984, 105:93–104
28. Brunt EM, Janney CG, Di Bisceglie AM, Neuschwander-Tetri BA, Bacon BR: Nonalcoholic steatohepatitis: a proposal for grading and staging the histological lesions. Am J Gastroenterol 1999, 94:2467–2474
29. Roskams T, Desmet V: Ductular reaction and its diagnostic significance. Semin Diagn Pathol 1998, 15:259–269
30. Koteish A, Yang S, Lin H, Huang, Diehl AM: Ethanol induces redox-sensitive cell-cycle inhibitors and inhibits liver regeneration after partial hepatectomy. Alcohol Clin Exp Res 2002, 26:1710–1718
31. Lowes KN, Brennan BA, Yeoh GC, Olynyk JK: Oval cell numbers in human chronic liver diseases are directly related to disease severity. Am J Pathol 1999, 154:537–541
32. French SW, Ruebner BH, Mezey E, Tamura T, Halsted CH: Effect of chronic ethanol feeding on hepatic mitochondria in the monkey. Hepatology 1983, 3:34–40
33. Yeldandi AV, Rao MS, Reddy JK: Hydrogen peroxide generation in peroxisome proliferator-induced oncogenesis. Mutat Res 2000, 448: 159–177
34. Torbenson M, Yang SQ, Liu HZ, Huang J, Gage W, Diehl AM: STAT-3 overexpression and p21 up-regulation accompany impaired regeneration of fatty livers. Am J Pathol 2002, 161:155–161
35. De Vos R, Desmet V: Ultrastructural characteristics of novel epithelial cell types identified in human pathological liver specimens with chronic ductular reaction. Am J Pathol 1992, 140:1441–1450
36. Ros J, Libbrecht L, Geuken M, Jansen P, Roskams T: High expression of MDR1, MRP1 and MRP3 in the hepatic progenitor cell compartment and hepatocytes in severe human liver disease. J Pathol 2003, 200:553–560
37. Renes J, de Vries EE, Hooiveld GJ, Krikken I, Jansen PL, Muller M: Multidrug resistance protein MRP1 protects against the toxicity of the major lipid peroxidation product 4-hydroxynonenal. Biochem J 2000, 350:555–561